

A Comparison of Jaw Dimensional and Quality Assessments of Bone Characteristics with Cone-Beam CT, Spiral Tomography, and Multi-Slice Spiral CT

Miet Loubele¹/Maria Eugenia Guerrero²/Reinhilde Jacobs^{3,4}/Paul Suetens³/Daniel van Steenberghe^{4,5}

Purpose: For proper preoperative planning of oral implants, the need has increased for tomographic imaging for precise determination of anatomic dimensions. However, concern for radiation exposure, which is substantial with computerized tomography (CT), has also grown. In the present study, the validity of jawbone width assessment and delineation by means of cone-beam CT (CBCT) and spiral tomography on dry mandibles was compared. Secondly, the subjective image quality of CBCT images with those obtained by multi-slice spiral CT (MSCT) of a fixed ex vivo cadaver with its soft tissues was compared. **Materials and Methods:** The study included 25 dry human mandibles for the dimensional study and 1 formalized maxilla for image quality assessment. Measurements of the mandibles by means of a digital sliding caliper acted as the gold standard. Radiographic examination of the premolar and canine regions was performed with both CBCT and spiral tomography. Observational measurements were carried out by postgraduates in oral imaging. Subjective image quality was assessed on the fixed maxilla, including soft tissues, by comparing CBCT and MSCT. Inter- and intraobserver variability were determined. **Results:** Direct mandibular measurements were on average 0.23 mm (SD 0.49) and 0.34 mm (SD 0.90) larger than the CBCT and spiral tomography measurements, respectively. Subjective image quality of the CBCT was significantly better than for the MSCT with regard to visualization and delineation of the lamina dura and periodontal ligament space. Subjective image quality of the MSCT was significantly better for the MSCT than the CBCT for the gingiva and cortical bone. **Conclusions:** These results indicate that on dry mandibles, jawbone width measurements by means of CBCT and spiral tomography are reliable, even if on average they slightly underestimate the bone width. For the subjective image quality, the CBCT offered better visualization of details of the small bony structures. Spiral tomography offered better visualization of the cortical bone and the gingiva. *INT J ORAL MAXILLOFAC IMPLANTS* 2007;22:446-454

Key words: computerized tomography, cone-beam computed tomography, dental implants, jawbone, preoperative planning, 3-dimensional imaging

¹PhD Student, ESAT-PSI, Medical Imaging Center, Katholieke Universiteit Leuven, Belgium.

²Master Student, Department of Periodontology, School of Dentistry, Oral Pathology and Maxillofacial Surgery, Katholieke Universiteit Leuven, Belgium; Oral Imaging Center, School of Dentistry, Oral Pathology and Maxillofacial Surgery, Katholieke Universiteit Leuven, Belgium.

³Professor, ESAT-PSI, Medical Imaging Center, Katholieke Universiteit Leuven, Belgium.

⁴Professor, Department of Periodontology, School of Dentistry, Oral Pathology and Maxillofacial Surgery, Katholieke Universiteit Leuven, Belgium.

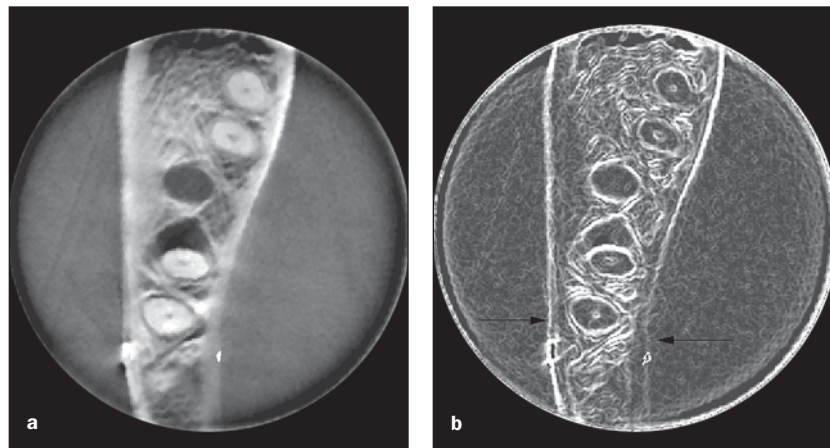
⁵P-I Brånemark Chair in Osseointegration, Department of Periodontology, School of Dentistry, Oral Pathology and Maxillofacial Surgery, Katholieke Universiteit Leuven, Belgium.

Correspondence to: Dr Reinhilde Jacobs, Oral Imaging Center, School for Dentistry, Oral Pathology and Maxillofacial Surgery, Katholieke Universiteit Leuven, Kapucijnenvoer 7, B-3000 Leuven, Belgium. Fax +32 16 332410. E-mail: Reinhilde.Jacobs@uz.kuleuven.be

Multi-slice computerized tomography (MSCT) provides data in a 3-dimensional (3D) format offering information on craniofacial anatomy for diagnosis and for the planning of oral implant placement. Several reports have demonstrated the clinical advantages of using MSCT scanning, especially when combined with 3D implant-planning software.¹ This technology enables the virtual placement of implants in a 3D model of the patient's jaw.¹

Unfortunately, the use of MSCT results in significantly higher absorbed radiation doses than panoramic radiography or linear tomography.² With MSCT, a fan-beam x-ray is transmitted from the source to a 1-dimensional detector, both of which are affixed to a rotating gantry. Several rotations of the gantry around the patient are needed for image acquisition. The need for less expensive image acquisition protocols or scanners with lower radiation doses has led to the development of techniques

Fig 1 Cross-sectional images of a mandible obtained using CBCT with (a) the Hi Pass filter and (b) the Edge filter. Bone delineation is not clear at the lingual aspect of canine or premolar regions (arrows), but the buccal cortex is clearly delineated.



such as cone-beam computerized tomography (CBCT).²⁻⁴ *Cone-beam computerized tomography* is so called because the x-ray forms the shape of a cone. This cone-beam x-ray is transmitted from the source to a 2-dimensional detector which is, together with the source, fixed on a rotating gantry and rotated 360 degrees (ie, only a single rotation is required).

Currently 4 CBCT scanners dominate the market: NewTom 3G (Quantitative Radiology, Verona, Italy), Accuitomo 3D (Morita, Kyoto, Japan), I-CAT Cone Beam 3-D Dental Imaging System (I-CAT Imaging Sciences International, Hattfield, PA), and MercuRay CB (Medico Technology, Kashiwa, Japan). In this paper the Accuitomo 3D will be evaluated. This CBCT has the smallest field of view (FOV) of the available CBCT devices, 4 cm in diameter and 3 cm in height. It is able to acquire high-resolution images while delivering a high radiation dose only to the area within the FOV and tissue in close proximity to the FOV. The device is compact and affordable, and it uses comparable hardware to the panoramic apparatus. The patient can sit in a chair during image acquisition. Thus, CBCT can be of great value with regard to the planning of oral implants in cases of partial edentulism, where the use of a classical CT often seems questionable.^{5,6}

Disadvantages are the radiation scatter,⁷ the limited dynamic range of the x-ray area detectors, the truncated-view artifact,⁷ and artifacts caused by beam hardening. The truncated view artifact can be noticed as a white edge at the border of the FOV. Beam hardening results in lower-intensity imaging of the jawbone at the posterior lingual side of the mandible and maxilla. These drawbacks may influence image quality. Therefore, studies are needed to evaluate the effect of these artifacts on image quality in, for example, the field of oral implant placement. Because pilot studies have demonstrated difficulties with the bone segmentation in these images, the question that the

present investigators sought to resolve was the subjective image quality of the 2D slices.

The Accuitomo is compared with the 2 main hardwares available in oral health care in 2 studies. The first study compares the validity of jawbone width assessment and delineation by means of CBCT and spiral tomography on dry mandibles. The second study compares the subjective image quality of CBCT images of a fixed ex vivo cadaver with its soft tissues with those obtained by MSCT.

MATERIALS AND METHODS

Study 1: Delineation of the Bone

Aim of the Study. The aim of this study was to investigate the delineation of the bone contour and to determine any relation between bone thickness or inclination of the bone and the results obtained with CBCT and spiral tomography. Because the posterior region of the mandible suffers the most from the beam-hardening artifact, delineation of the canine and the posterior region was evaluated (Fig 1).

Phantom Selection and Preparation. Twenty-five dry mandibles of Indian origin were examined. These mandibular bone specimens came from patients who had donated their bodies for research and were kindly provided from the Department of Morphology University Centre (Hasselt, Diepenbeek, Belgium). Fully and partially edentulous mandibles were selected. Gutta-percha (Obtura II; Spartan Co, Fenton, MO) was used to fabricate small radiographic markers, which were glued on the buccal and lingual aspects of the sites of the mandible selected for scanning. For tomographic images, the size of the gutta-percha points was increased to 2 mm. During image acquisition, the mandibles were always positioned the same way to obtain comparable images of the region of interest, with the x-ray beam coincid-

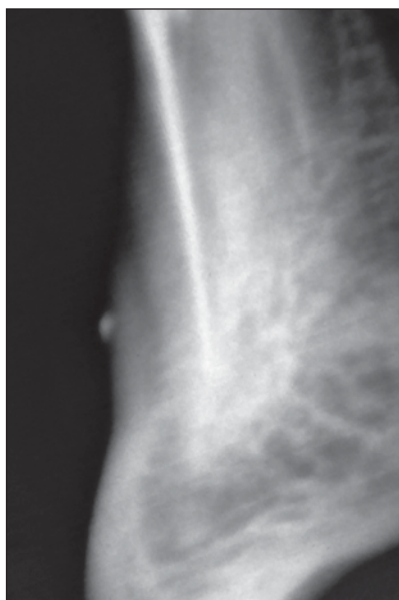


Fig 2 Cross-sectional image of the canine region acquired with spiral tomography.

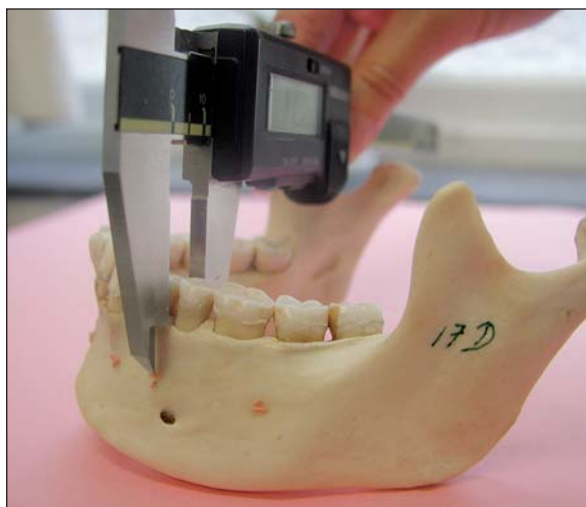


Fig 3 Macroscopic examination of the thickness of mandibular bone at the gutta-percha markers level using a digital caliper with a 0.01-mm resolution.

Table 1 Subjective Image Quality Determined Using a 4-point Rating Scale

1	Impossible to observe delineation of the bone contour
2	Difficult to observe delineation of the bone contour
3	Probably possible to visualize delineation of the bone contour
4	Definitely possible to visualize delineation of the bone contour

ing with the line connecting the 2 gutta-percha points. To simulate soft tissues, mixD was used. This consists of a mixture of paraffin, polyethylene, magnesium oxide, and titanium oxide which is well-known to be adequate for soft tissue simulation.⁸ In addition, a “cervical spine” and a bottle of water were adapted to absorb some secondary radiation.

Scanning. For the Accuitomo 3D, the images were scanned with a tube voltage of 70 kVp, a tube current of 2mA, and a scanning time of 17.5 seconds. The spiral tomography examination was performed with a Cranex TOME (Soredex Orion, Helsinki, Finland). Two tomographic films were obtained, 1 from the canine and the other from the premolar region of each dry mandible. Four tomographic slices were obtained from each specimen; the slice with the sharpest gutta-percha point was selected (Fig 2). The tomographic program for the mandible was selected at 57 kV, 1 mA, and 56 seconds. The layer thickness was set at 2 mm, and the aperture number at 4. Furthermore, images were produced using storage phosphor plates (Vistascan; Dürr-Dental, Bietigheim, Germany).

As a gold standard, bone-thickness measurements were performed at the fiducial marker level on the mandibles using a Mitutoyo digital sliding caliper (Mitutoyo, Andover, UK) with an accuracy of 0.01 mm (Fig 3).

Radiographic Observer Measurements. An observer with postgraduate education in oral imaging and experience in jawbone assessment measured both the lengths between the gutta-percha markers on the spiral tomographic and CBCT scans. With various image-processing functions, the i-Dixel software provided by Morita was used to measure the width and the angular measurements of the inclination of the bone at the premolar site (Figs 4 and 5) for the CBCT images.

On the spiral tomography images, measurements of the thickness of the bone were calculated on the DBSWIN software (Dürr-Dental). The examiner used her clinical judgment to delineate the bone from the surroundings at each side of the jawbone and to perform the measurement. Furthermore, the delineation of the bone was scored on the premolar and canine region using a 4-point rating scale (Table 1).

Statistical Analysis. Statistical analysis was performed using MedCalc 8.1.1 (MedCalc Software, Mariakerke, Belgium) and Microsoft Excel (Microsoft, Redmond, WA). Differences between the real bone measurements (gold standard) and the various radiographic films were determined using a paired 1-tailed *t* test, with $P < .05$ regarded as significant. Values obtained from the tomographic images were corrected according to their magnification factor.

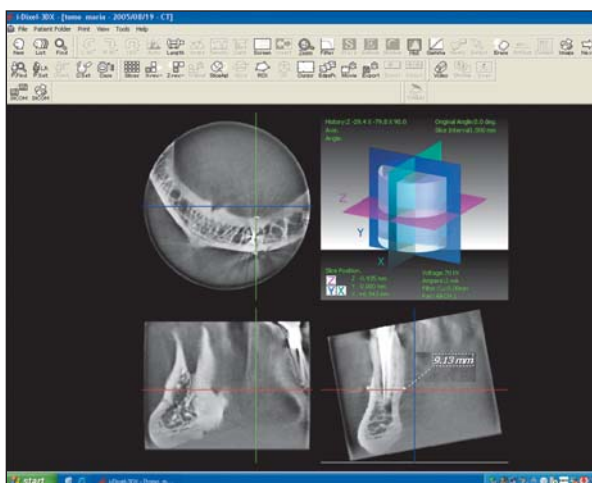


Fig 4 The lower righthand image shows measurement of the bone thickness at the fiducial markers in the canine region by the iDixel software.

All measurements were performed twice with a 1-month interval to allow evaluation of intraobserver variability. This intraobserver variability was calculated by the interclass correlation (ICC), the Spearman rank coefficient, and the coefficient of variation. The intraobserver agreement for the impression of the delineation was calculated with weighted kappa.

To determine whether the observer could judge the accuracy of her measurement, a scatterplot was made between the absolute difference and the impression of the bone delineation. Another scatterplot was made to examine the relation between the angle measurements and the absolute difference between the CBCT and caliper measurements.

Study 2: Evaluation of Subjective Image Quality

Aim of the Study. Three-dimensional CT scanning typically enables not only reliable dimensional assessment but also the evaluation on 2D slices of aspects such as the degree of corticalization or mineralization of the trabecular bone. Thus, the subjective image quality of 2D slices created by MSCT and CBCT scanning was also evaluated.

Phantom Selection and Preparation. The study material for the second study included 1 maxilla excised from a formalin-fixed cadaver donated for anatomy classes and research. This phantom was prepared following the Procera procedure.¹ Impressions were made to enable fabrication of the radiographic templates. One-millimeter holes were prepared, and 6 fiducial markers were placed in the templates. The holes were filled with warm gutta-percha (Obtura II).

Scanning. The specimen was scanned by both MSCT (Somatom Volume Zoom 4-slice CT scanner; Siemens, Erlangen, Germany) and CBCT (3D Accuitemo) at the partially edentulous sites. The exposure

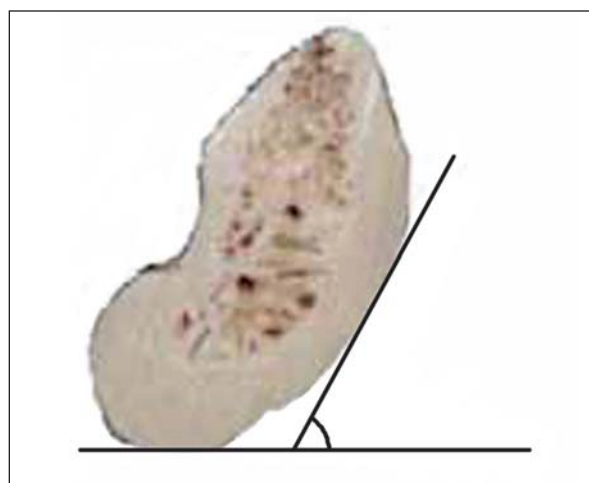


Fig 5 Cross-sectional image showing the angle made between a tangent to the lingual cortex and a tangent to the inferior border of the mandible.

Table 2 Settings for CT Scan Examination with the MSCT

Specification	Value
Tube voltage	120 kV
Tube current	90 mA
Collimation	2 × 0.5 mm
Feed/rotation	1 mm
Rotation time	0.75 s
Slice width	0.5 mm
Slice thickness	0.3 mm
Pixel size	0.363 × 0.363 mm
Reconstruction filter	H60s
Table feed	3 mm/s

protocol used for MSCT scanning is given in Table 2. The axial plane was positioned parallel to the hard palate of the maxilla. The scanning parameters for the CBCT scanner were 75 kVp, 4mA, and 17.5 seconds of exposure time.

Registration Between the MSCT and the CBCT Images. To be able to compare the subjective image quality, the same slices of the MSCT and the CBCT images needed to be evaluated. These slices were selected with custom-made software. First, a transformation was calculated which matched both volumes acquired with the CBCT and with the MSCT based on maximization of mutual information.⁹ Of the CBCT images, some axial, frontal slices were selected. Based on the calculated transformation, the same slice could be selected from the MSCT scan. The images were calculated based on linear interpolation. Because the MSCT scanner showed more information than the CBCT scanner, this part of the MSCT images was blacked out on the image so that comparison only could be made solely based on the information shown in both images.



Fig 6 A CBCT slice. Note the good visibility of the lamina dura, periodontal ligament space, and trabecular bone.

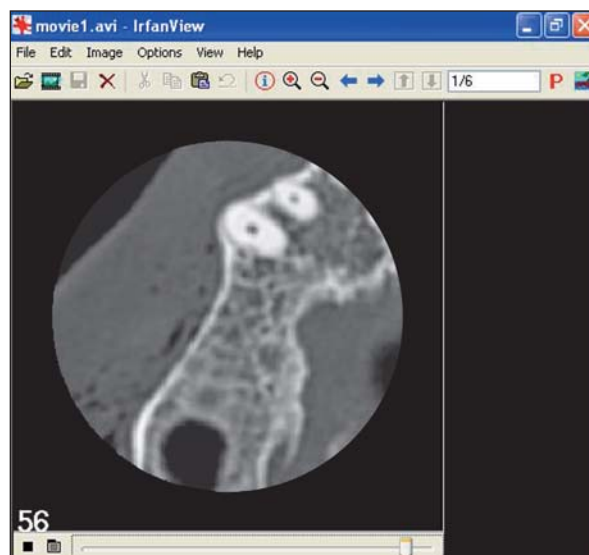


Fig 7 An MSCT slice. In this image, differentiation between lamina dura and periodontal ligament is very difficult.

The slices of the CBCT images and the MSCT images were visualized with the Image Processing Toolbox of Matlab R14. These were converted to TIFF (tagged image file format) without compression. Five random orders of the images were generated. With this random order of the images, a movie was created (Figs 6 and 7). These movies were converted to AVI (audio video interleave) format, again without compression. The movies were displayed on a 17-inch monitor with a screen resolution of $1,024 \times 764$ pixels and highest color quality 32 bits, with the viewing software IrfanView (freeware). The "full screen" option and the display option "fit window to image" were selected.

Radiographic Observer Measurements. After calibration sessions, 5 independent observers, postgraduates in oral imaging, assessed subjective image quality. One of the observers saw her movie twice with an interval of 1 week separating the viewings to assess intraobserver variability. The following structures were assessed: cortical bone, trabecular bone, lamina dura, periodontal ligament space, pulp cavity, dentin, and gums. Overall impressions of images were rated on the basis of their visibility, ranging from 1 (impossible to observe the landmark) to 4 (definitely possible to visualize the landmarks) (Table 1).

Statistical Analysis. The comparison of the subjective image quality was performed by applying a Wilcoxon signed rank test to the mean values of the observations of the different anatomic structures. In consideration of the small number of measurements, observers who were significantly less experienced with the imaging modality were excluded from the statistical analysis to avoid bias.

RESULTS

Study 1: Delineation of the Bone

The results of the measurements performed in the first study are summarized in Table 3. The ICC and the Pearson correlation showed good intraobserver agreement, and for the impression of the delineation a moderate intraobserver agreement was achieved (Table 4). This resulted in the differences summarized in Table 5. Regarding Table 5, the radiographic measurements were significantly smaller than the caliper measurements if $P \leq .05$. However, the interquartile distance for the difference between the CBCT measurements and the caliper measurements was much smaller than the differences between the spiral tomography measurements and the caliper measurements (Fig 8).

Based on the relationships between angular measurements, and the difference between the CBCT and caliper measurements (Figs 9 and 10), no significant correlation was established between the accuracy of the measurements and the quality of the bone delineation or between the angular measurements and the accuracy of the measurements.

Evaluation of Subjective Image Quality

The results of the second study are shown in Table 6. Based on this table, it could be concluded that observer 1 was not experienced with the perception of trabecular bone and periodontal ligament space on MSCT images. It could also be concluded that observer 3 was not experienced with the perception of the periodontal ligament space on MSCT images.

Table 3 Measurements Performed on the Dry Mandible by the Observer at the 2 Time Periods

Measurement	First observation			Second observation			Average		
	Mean	SD	95% CI	Mean	SD	95% CI	Mean	SD	95% CI
Caliper									
Linear (mm)	10.75	1.12	10.26, 11.24	10.76	1.08	10.29, 11.24	10.75	1.10	10.27, 11.23
CBCT									
Linear (mm)	10.51	1.15	9.97, 11.05	10.54	1.20	10.01, 11.07	10.53	1.17	10.01, 11.04
Angle (degrees)	73.46	8.32	69.81, 77.10				73.46	8.32	69.81, 77.10
Delineation*	2.45	0.89	2.06, 2.84	2.25	0.85	1.88, 2.62	2.35	0.84	1.98, 2.72
Spiral tomography									
Linear (mm)	10.44	1.14	9.94, 10.94	10.38	1.00	9.94, 10.82	10.41	1.07	9.94, 10.88

For each measurement, the mean, standard deviation (SD), and the 95% CI are given. For the intraobserver measurements, the weighted kappa is calculated for the impression of the delineation and for the other measurements the 95% CI is given. Angle was not calculated for the second observation. *Rating on a scale from 1 to 4 (Table 2) of the degree to which it was possible to observe the delineation of the bone contour.

Table 4 Evaluation of the Intrarater Agreement of the Different Measurements

	Pearson r	ICC or kappa	95% CI	CV (%)
Caliper (linear)	0.983	0.983	0.962, 0.992	1.96
CBCT (linear)	0.985	0.968	0.930, 0.985	1.96
CBCT (delineation)		0.778		
Spiral tomography (linear)	0.988	0.964	0.921, 0.983	1.77

CV = coefficient of variation.

For the linear measurements, the Pearson correlation coefficient was calculated. For the intrarater agreement, the weighted kappa value was calculated. For the Pearson correlation coefficient, the 95% CI is displayed.

Table 5 Overview of the Differences Between the Different Measurements

Measurement	First observation				Second observation				Global			
	Mean	SD	95% CI	P	Mean	SD	95% CI	P	Mean	SD	95% CI	P
CBCT-caliper	-0.24	0.40	-0.06, 0.42	.008	-0.21	0.58	-0.04, 0.47	.058	-0.23	0.49	-0.01, 0.44	.0526
Spiral-caliper	-0.32	0.94	-0.76, 0.12	.075	-0.38	0.88	-0.79, 0.03	.036	-0.34	0.90	-0.77, 0.08	.0522
CBCT-MSCT	0.105	1.01	-0.37, 0.58	.32	0.13	1.13	-0.40, 0.66	.300	-0.12	1.07	-0.38, 0.62	.31
Spiral-CBCT	-0.09	1.11	-0.61, 0.43	.36	-0.152	1.03	-0.63, 0.33	.260	-0.12	1.07	-0.62, 0.38	.31

For each row X-Y the different measurements of X are compared with the mean value of Y. For each comparison, the mean and the standard deviation, the 95% CI of the mean, and the P-value for being scientifically smaller are given. Spiral = spiral tomography.

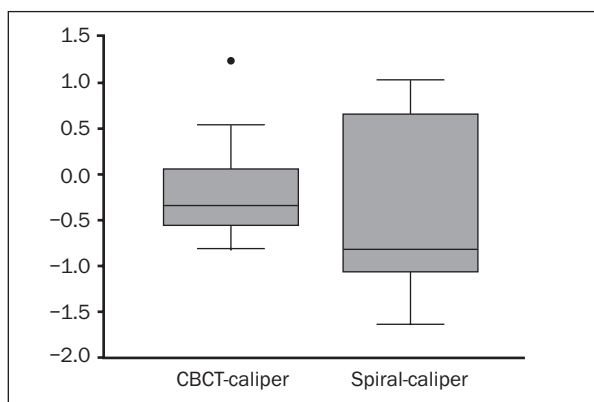


Fig 8 Box plots of the differences between the mean radiographic measurements and the mean caliper measurements are shown in mm. Spiral = spiral tomography.

Therefore, these 2 observers were not included in the statistical analysis for these items. After these corrections, the final data for this study can be found in Table 7. From this table, it can be concluded that cortical bone and gingiva can be perceived better on MSCT than CBCT ($P < .05$). The lamina dura and the periodontal ligament space can be perceived better on the CBCT images. For the pulp, the dentin, and the trabecular bone, no significant difference existed. When the threshold for a good judgment is set at 2.5, all the structures were sufficiently visible except for the periodontal ligament space in the MSCT images and the lamina dura. The mean of all observational scores was 2.5. Due to the small sample size, no kappa values could be calculated.

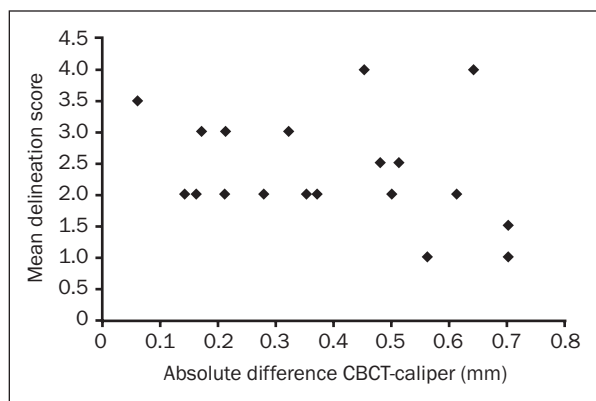


Fig 9 Scatterplot of the relation between the absolute difference between the CBCT and the caliper measurements and the mean delineation score.

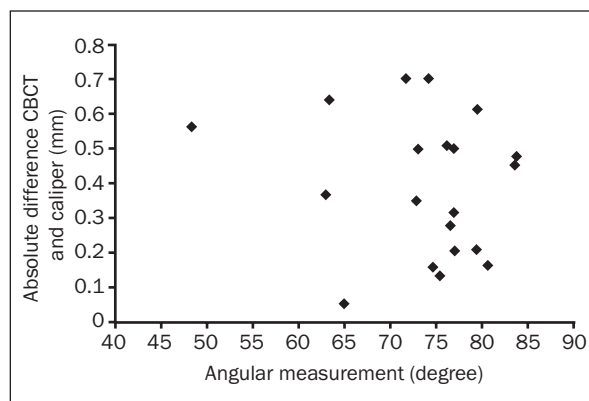


Fig 10 Scatterplot of the relation between the angular measurements and the absolute difference between CBCT and caliper measurements.

DISCUSSION

Recent therapeutic options in periodontal and oral surgery in general are codependent on precise diagnostic imaging. Ensuring radiographs of consistently acceptable quality is obviously of benefit to the patient and the clinician. It is especially important when oral implants have to be planned in anatomic areas where bone width is limited. Accurate assessment can be the difference between immediate implant placement and the ability to place implants only after bone augmentation. While a jawbone width of at least 4 mm allows the insertion of many available implant types, this is not so for a jawbone width 3 mm. Thus, precision up to the millimeter level is crucial.

Partial edentulism is a prominent indication for the use of oral implants. The imaging of such limited areas may not need to involve a relatively cumbersome and expensive CT examination, which often results in radiation exposure of areas outside the region of interest. With CBCT, the tissues involved are limited to a smaller volume.

The comparison between the CBCT, spiral tomography, and real measurements revealed reliable results for both imaging modalities. The small differences between the image modalities were due to differences in delineation of bone volume. Clinically, one should be more concerned with overestimation which are more frequent with spiral tomography and reached up to 1 mm. With CBCT, bone width was overestimated by only 0.5 mm except for 1 outlier.

Both devices presented statistically significant underestimations, which would lead to a too-prudent clinical decision. CBCT observations are in agreement with previous findings.¹⁰⁻¹⁴ Presumably this was due to a partial volume and segmentation

algorithm effect. According to Bou Serhal et al,¹² image quality on spiral tomography can be influenced by different factors, such as ability of the operator and patient positioning. In the present study, the lower border of the mandible was always in a horizontal plane to offer the best image definition.

The good intraobserver agreement obtained in this study may be attributed to the familiarity of the observers to this technique and their radiographic skills. Of course one cannot extrapolate these optimistic findings to the clinical level, where soft tissues further blur the images obtained.

When analyzing image quality, the cone beam offers high resolution in any direction. The 0.125-mm cubic voxels of the 3D Accuitomo contributed to the high resolution of all section images. Usually, the Somatom Volume Zoom 4-slice CT scanner has a voxel size of 0.363 mm. Thus, for oral applications, the axial section images of the MSCT scanner achieve relatively high resolution, but its multiplanar reconstruction images are of low resolution.¹¹ Actually, the resolution of spiral tomography images (other than axial-section images) is usually insufficient for the observation of trabecular bone and periodontal ligament space.

The quality of CT images is affected by the scanning settings. Several combinations of the slice thickness, slice interval, and tube current can influence image quality. Kim et al¹⁵ reported that a thin slice appeared to help establish more accurate 3D CT cranial measurements when a human skull phantom was used. In this investigation, spiral tomography with axial slices with a width of 0.5 mm was used to optimize results.

Moreover, image quality can be objectively qualified by measuring noise, resolution, and contrast.¹⁴ Previous authors have pointed out that image noise increases with a reduction in radiation dose.^{16,17}

Table 6 Overview of the Mean Score (1 to 4) of the Different Anatomic Structures for MSCT and CBCT for Each Observer and All Observers as a Group (Global)

	Observer 1 ¹		Observer 1 ²		Observer 2		Observer 3		Observer 4		Observer 5		Global	
	MS	CB	MS	CB	MS	CB	MS	CB	MS	CB	MS	CB	MS	CB
Axial														
Trabecular bone	2.1	3.9	2.6	3.9	4.0	4.0	3.9	3.6	3.3	4.0	3.8	3.9	3.3	3.9
Cortical bone	3.9	3.8	3.9	3.4	4.0	4.0	3.8	3.5	4.0	3.7	3.8	3.9	3.9	3.7
Lamina dura	1.3	3.8	1.5	3.8	2.6	3.7	1.8	3.6	2.6	4.0	3.3	4.0	2.2	3.8
Periodontal ligament	1.1	3.6	1.4	3.8	2.9	3.6	1.8	3.4	2.1	4.0	2.5	4.0	2.0	3.7
Pulp	4.0	4.0	4.0	4.0	4.0	4.0	4.0	4.0	4.0	4.0	4.0	4.0	4.0	4.0
Dentin	3.9	4.0	3.9	3.9	4.0	4.0	4.0	3.9	4.0	4.0	4.0	4.0	4.0	4.0
Gingiva	3.8	3.8	4.0	3.4	4.0	4.0	2.6	2.4	4.0	3.6	2.4	3.6	3.5	3.4
Frontal														
Trabecular bone	1.9	3.1	2.4	3.0	3.7	3.6	3.0	3.4	3.4	3.3	3.8	3.3	3.0	3.3
Cortical bone	3.7	3.9	3.1	3.4	4.0	3.9	4.0	3.7	3.7	2.7	4.0	3.8	3.8	3.6
Lamina dura	1.1	2.4	2.1	3.0	2.4	2.3	2.7	3.0	3.0	3.6	2.7	2.8	2.3	2.8
Periodontal ligament	1.1	2.3	2.3	2.7	2.4	2.0	2.1	2.9	2.7	3.3	2.0	1.8	2.1	2.5
Pulp	4.0	3.7	4.0	4.0	4.0	4.0	3.1	3.6	3.6	3.4	3.3	3.5	3.7	3.7
Dentin	4.0	3.9	4.0	4.0	4.0	4.0	4.0	3.9	4.0	4.0	4.0	4.0	4.0	4.0
Gingiva	4.0	3.4	3.9	3.3	4.0	4.0	3.7	3.1	4.0	3.7	3.0	2.5	3.8	3.3
Axial + Frontal														
Trabecular bone	2.0	3.5	2.5	3.5	3.9	3.8	3.5	3.5	3.4	3.6	3.8	3.7	3.2	3.6
Cortical bone	3.8	3.8	3.5	3.4	4.0	3.9	3.9	3.6	3.9	3.2	3.9	3.7	3.8	3.6
Lamina dura	1.2	3.1	1.8	3.4	2.5	3.0	2.2	3.3	2.8	3.8	3.0	3.5	2.3	3.4
Periodontal ligament	1.1	3.0	1.8	3.3	2.7	2.8	1.9	3.1	2.4	3.6	2.3	3.1	2.0	3.2
Pulp	4.0	3.9	4.0	4.0	4.0	4.0	3.6	3.8	3.8	3.7	3.7	3.8	3.9	3.9
Dentin	3.9	3.9	3.9	3.9	4.0	4.0	4.0	3.9	4.0	4.0	4.0	4.0	4.0	4.0
Gingiva	3.9	3.6	3.9	3.3	4.0	4.0	3.1	2.7	4.0	3.6	2.6	3.0	3.6	3.4

Table 7 Subjective Image Quality—Final Data

	Observers	MSCT		CBCT		P*
		Mean	SD	Mean	SD	
Trabecular bone	2, 3, 4, 5	3.6	0.5	3.7	0.6	.39
Cortical bone	1, 2, 3, 4, 5	3.8	0.4	3.6	0.4	.04
Lamina dura	1, 2, 3, 4, 5	2.2	0.5	3.4	0.7	< .001
Periodontal ligament	2, 4, 5	2.5	0.5	3.2	0.9	.04
Pulp	1, 2, 3, 4, 5	3.9	0.3	3.8	0.3	.81
Dentin	1, 2, 3, 4, 5	4.0	0.1	4.0	0.1	> .99
Gingiva	1, 2, 3, 4, 5	3.6	0.3	3.3	0.4	.01

*Wilcoxon signed rank test.

Hence, image noise of CBCT has been assessed to be higher than that of conventional helical CT. The present study shows that slightly noisier images were acquired with the 3D Accuitomo compared with the Somatom Volume Zoom 4-slice CT scanner.

Metallic components in the region of interest or in the immediate vicinity can create a lot of artifacts. However, this is not a major limitation because such artifacts may be eliminated by metal artifact-reduction software. Furthermore, artifacts resulting from crowns, prostheses, or metal fillings could be avoided by starting the data acquisition inferior to the level of the dental crowns.

Additionally, the selection of the correct filter during CT acquisition can reduce noise. The selection of the H60s as the reconstruction filter was part of the CT dental protocol suggested by Siemens, as this filter gives nice bone segmentation. The U90u filter, which is also commonly used, leads to sharper but noisier images and gives a much higher radiation dose for a limited area of the maxillofacial region. The presence of such noise demands a longer time to generate a model and the need for a smoothing technique. Smoothing implies the risk of reducing details and moving arbitrarily the boundaries of the bone segmentation. Thus, the choice of H60s was logical for this application.

In the present investigation, the raw images were not viewed, since the intention was to compare the use of the CBCT with MSCT for oral implant planning. The software for such planning involves reformatting of the dataset.

In addition, it has been stated that the great advantage of CT is that one can depict soft tissue as well as bony structures on the same scan.^{18,19} In the present study, the visualization of soft tissues was more difficult with CBCT because of the low contrast resolution. This is demonstrated by the fact that the gingiva could be seen better in the MSCT than in the CBCT images.

Bone segmentation was less clear in the CBCT images due to poor image quality. The noise was also increased by the thin slice width used in the experiments. This thin slice width was needed for the fusing of the 2 images generated by the double-scan procedure of ProCera.¹ Better image quality might be obtained with new software recently obtained for the 3D Accuitomo.

CONCLUSIONS

The present study showed that both CBCT and spiral tomography images allowed for accurate dimensional measurements in the premolar region on dry mandibles. These imaging modalities are suitable for visualizing and measuring the width of the potential implant sites if one accepts overestimations of a maximum of 1 mm for spiral tomography and 0.5 mm (with 1 exception) for the CBCT.

On average, both devices underestimate the jawbone width.

Bone thickness did not influence good delineation of the bone at the premolar site. Further research on a better segmentation algorithm may further improve the acquired results. Lamina dura and periodontal ligament space could be better perceived on CBCT; cortical bone and gingiva could be better perceived on MSCT.

REFERENCES

1. van Steenberghe D, Naert I, Andersson M, Brajnovic I, Van Cleynbreugel J, Suetens P. A custom template and definitive prosthesis allowing immediate implant loading in the maxilla: A clinical report. *Int J Oral Maxillofac Implants* 2002;17:663–670.
2. Hamada Y, Kondoh T, Noguchi K, et al. Application of limited cone beam computed tomography to clinical assessment of alveolar bone grafting: A preliminary report. *Cleft Palate Craniofac J* 2005;42:128–137.
3. Tsiklakis K, Syriopoulos K, Stamatakis HC. Radiographic examination of the temporomandibular joint using cone beam computed tomography. *Dentomaxillofac Radiol* 2004;33:196–201.
4. Pawelzik J, Cohnen M, Willers R, Becker J. A comparison of conventional panoramic radiographs with volumetric computed tomography images in the preoperative assessment of impacted mandibular third molars. *J Oral Maxillofac Surg* 2002;60:979–984.
5. Bou Serhal C, Jacobs R, Quirynen M, van Steenberghe D. Imaging technique selection for the preoperative planning of oral implants: A review of the literature. *Clin Implant Dent Relat Res* 2002;4:156–172.
6. Cohnen M, Kemper J, Möbes O, Pawelzik J, Mödder U. Radiation dose in dental radiology. *Eur Radiol* 2002;12:634–637.
7. Mozzo P, Procacci C, Tacconi A, Martini PT, Andreis IA. A new volumetric CT machine for dental imaging based on the cone-beam technique: Preliminary results. *Eur Radiol* 1998;8:1558–1564.
8. Chen CZ. The making of a body phantom device with MIXDp and MIXD [author's transl]. *Zhonghua Fang She Xue Za Zhi* 1980;14:306–307.
9. Maes F, Collignon A, Vandermeulen D, Marchal G, Suetens P. Multimodality image registration by maximization of mutual information. *IEEE Trans Med Imaging* 1997;16:187–198.
10. Lascala CA, Panella J, Marques MM. Analysis of the accuracy of linear measurements obtained by cone beam computed tomography (CBCT-NewTom). *Dentomaxillofac Radiol* 2004;33:291–294.
11. Peltola JS, Mattila M. Cross-sectional tomograms obtained with panoramic radiographic units in the assessment of implant site measurements. *Dentomaxillofac Radiol* 2004;33:295–300.
12. Bou Serhal C, van Steenberghe D, Quirynen M, Jacobs R. Localization of the mandibular canal using conventional spiral tomography: A human cadaver study. *Clin Oral Implants Res* 2001;12:230–236.
13. Arai Y, Tammissalo E, Iwai K, Hashimoto K, Shinoda K. Development of a compact computed tomographic apparatus for dental use. *Dentomaxillofac Radiol* 1999;28:245–248.
14. Hashimoto K, Arai Y, Iwai K, Araki M, Kawashima S, Terakado M. A comparison of a new limited cone beam computed tomography machine for dental use with a multidetector row helical CT machine. *Oral Surg Oral Med Oral Pathol Oral Radiol Endod* 2003;95:371–377.
15. Kim DO, Kim HJ, Jung H, Jeong HK, Hong SI, Kim KD. Quantitative evaluation of acquisition parameters in three-dimensional imaging with multidetector computed tomography using human skull phantom. *J Digit Imaging* 2002;15(suppl 1):254–257.
16. van Daatselaar AN, van der Stelt PF, Weenen J. Effect of number of projections on image quality of local CT. *Dentomaxillofac Radiol* 2004;33:361–369.
17. Frederiksen NL. Health physics. In: White SC, Pharoah MJ. *Oral Radiology: Principles and Interpretation*, ed 5. St Louis: Mosby, 2004:255.
18. Nkenke E, Zachox S, Benz M, et al. Fusion of computed tomography data and optical 3D images of the dentition for streak artifact correction in the simulation of orthognathic surgery. *Dentomaxillofac Radiol* 2004;33:226–232.
19. Schulze D, Heiland M, Thurmann H, Adam G. Radiation exposure during midfacial imaging using 4- and 16-slice computed tomography, cone beam computed tomography systems and conventional radiography. *Dentomaxillofac Radiol* 2004;33:83–86.